Optomechanically Assisted Assembly of Surface-Functionalized Zeolite-L-Based Hybrid Soft Matter

Álvaro Barroso, Tim Buscher, Katrin Ahlers, Armido Studer,* and Cornelia Denz*

Nanoporous particles are particularly interesting for the assembly of functional nano- and microsystems because they provide hierarchical supramolecular organization of a large variety of guest molecules. In this work, arbitrary nanoarchitectures consisting of nanoporous zeolite-L crystals are assembled by combining holographic optical tweezers (HOT) with polymer brush functionalized particles to overcome the limitations of 1D and restricted self-assembly of zeolite-L crystals. Readily prepared and functionalized polymer shells allow for controlled, instant, and highly efficient particle–particle and particle–surface adhesion without the need for an external trigger. In contrast to earlier studies, these assemblies remain permanently stable after release out of the HOT system. This novel strategy can be used to fabricate either motile units or locally grounded 1D, 2D, and 3D microconstructions, which can be further utilized as microtools in microfluidic and nanophotonic applications.

Assembling components at the micro- and nanoscale in a reliable, reproducible, and automated way is still a technological challenge for the fabrication of functional materials and devices with applications in biomedicine and nanotechnology.[1] Colloidal assembly is a well-known strategy used for the construction of tailored microtools that are designed to perform specific tasks in research areas such as microfluidics, tissue engineering, and photonics engineering.[2] The efficiency of the assembly depends crucially on engineering the particle surface so that interparticle forces or molecular surface forces (van der Waals, electrostatic, magnetic, molecular, and entropic) responsible for the (self-)assembly process are fully controlled. Such molecular forces may be also used to obtain supramolecular assembly of molecules.[3] However, an alternative advantageous strategy to achieve hierarchical organization of molecules is to employ porous, internally nanostructured materials which, as host particles, can accommodate guest molecules within the particle nanochannels,[4] thereby creating a first stage of hierarchical order. On the one hand, the order and confinement exerted by the internal nanostructure of the particle can be exploited to enhance the properties of the molecular guests, leading to hybrid materials with efficient tailored functionalities. On the other hand, the nanocontainers themselves may be assembled at a second stage of hierarchical order into complex configurations, either assembling many elements of the same or of different species.[5,6] This allows constructing sophisticated microdevices, which feature a level of molecular organization that ranges from the molecular to the macroscopic scale. In this respect, the realization of large assemblies of nanocontainers demands the development of novel schemes that exploit and combine, on the one hand, methods for surface functionalization of these guest-nanochannels composites, and on the other hand, techniques that enable the assembly of microparticles into arbitrary 3D configurations. In the present work, we tackle this challenge by an original method based on zeolite-L crystals as a model system of nanocontainers, which are optomechanically assembled into arbitrary 3D microstructures after tailoring the crystal surface to provide specific interparticle forces.

Zeolite-L is a versatile inorganic nanoporous aluminosilicate that features a large number of strictly 1D aligned nanochannels (channel diameter: 0.71–1.26 nm) across the whole crystal axis,[7] in which they can accommodate a variety of guest molecules, as, e.g., organic dyes or drugs.[6,8] Due to their unique nanochannel properties, zeolite-L crystals have been used as building blocks of microsystems and microdevices for exciting photonic and biological applications, as, e.g., polarization sensors or bio-hybrid microrobots.[9–12] In addition, classical methods for silica particle modification can be used to modify the outer surface of zeolite-L to further tailor its properties. A broad variety of monolayers bearing basic functionalities such as reactive moieties, polymerization initiators, dyes, bio- and macromolecules, and proteins has been demonstrated.[13–17]

The initial technique of choice to assemble zeolite-L crystals into larger structures for hierarchical supramolecular organization was based on self-assembly.[14] Due to their particular morphology, zeolite-L crystals can be functionalized site-specifically at the pore entrances of the crystal's base area,[18,19] such that the resulting anisotropic reactivity can lead to linear self-assembly in solution when brought together with a dissolved complementary reactive crosslinker.[6,20] Moreover, complementary modified crystals may form chains with defined, alternating order.[6,21] Although very promising, these initial approaches showed low efficiency, while in addition the self-assembled zeolite-L crystals were limited to 1D structures.

Á. Barroso, K. Ahlers, Prof. C. Denz
Institute of Applied Physics
University of Muenster
Corrensstraße 2/4, 48149 Muenster, Germany
E-mail: denz@uni-muenster.de
Dr. T. Buscher, Prof. A. Studer
Organic Chemistry Institute
University of Muenster
Corrensstraße 40, 48149 Muenster, Germany
E-mail: studer@uni-muenster.de

1800041 (1 of 6)

In the past five years, more complex configurations, as, e.g., 2D and 3D reconfigurable assemblies have been demonstrated by using holographic optical tweezers (HOT).[22] This technique allows simultaneous optical trapping and manipulation of several zeolite-L crystals, yet the realized assemblies disassembled when being released from the trapping laser beam.

In a step further, the optomechanical assembly of individual zeolite crystals was considerably refined by appropriately setting the working conditions with respect to the chemical environment. For this purpose, an optical-tweezers assembly line based on the combination of HOT, microfluidics, and colloidal interactions was realized for the construction of permanent and functional 2D and 3D zeolite-L based microstructures with different geometrical complexity.[9] Despite its versatility to fabricate zeolite-L-based microstructures in 3D, the method requires the supply of several zeolite-L crystals from which typically only a few are used in a time-consuming assembly process. To overcome these limitations, we demonstrate herein an efficient design of larger functional systems by a versatile combination of selective chemical modification of the zeolite-L surface with subsequent optomechanically assisted linkage of individual crystals with HOT.

For this purpose, we employ zeolite-L based polymer brush particles, which can be readily functionalized in a modular way.[12] These zeolite-L/polymer hybrids feature a softer surface and higher density of functionalities in comparison to crystals modified with monolayers, and thus exhibit a higher capability to interact. In the recent past, there have been various approaches benefiting from these polymer hybrid systems in terms of particle self-assembly.[23–28]

In this report, we present two distinct approaches (A and B) based on different noncovalent interactions (**Figure 1**), both showing instant performance at room temperature in readily prepared dispersions. On the one hand, assemblies with hydrophobic surface properties and negative zeta potentials (ζ) will be realized. These aggregates do not adhere to the hydrophilic glass substrate surface and hence are suitable for the fabrication of motile microtools (approach A). On the other hand, partially hydrophilic particles with positively charged zeta potentials adhere to the glass substrate and thus are well suited as building blocks for the construction of locally grounded architectures (approach B). Altogether, this integral strategy represents an optical bottom-up counterpart to well-established photolithography and implicates several advantages in comparison with other laser-based micro3D printing techniques,[29–32] such as utilization of multifunctional building units and simultaneous incorporation of different materials.

Two types of zeolite-L crystals (≈1 and 4 µm in length, and both 1 µm in diameter) were utilized as the core building blocks for realizing polymer hybrid particles in order to demonstrate the applicability of our approach to different particle shapes and sizes. To assemble single particles into hierarchical structures following approach A, zeolite-L crystals were decorated with a hydrophobic polystyrene brush (chemical structure see **Figure 2**a). Estimated molecular weight (M_n) of the surface bound polymer strands is $M_n = 41$ kg mol^{-1} with a polydispersity index (Đ) of Đ = 1.13 (for 1 µm crystals) and $M_n = 62$ kg mol^{-1} with a Đ = 1.17 (for 4 µm crystals), respectively, as determined by gel permeation chromatography (GPC) analysis of unbound polymer, which was generated during the polymer brush synthesis.[12] Polystyrene brush particles show a negative zeta potential of $\zeta_{1\,\mu m} = -48.1$ mV and $\zeta_{4\,\mu m} = -59.0$ mV in ammonium formate buffer (AFB, 20×10^{-3} M, pH = 7.4, 25 °C).

Prior the experiments, zeolite-L/polymer core–shell particles were diluted in a solution of the polar aprotic solvent *N,N*-dimethylformamide (DMF) and sonicated for 10 min to achieve stable dispersion of single crystals. A small volume of the sample was pipetted between two thin glass coverslip for the realization of the experiments in the HOT system. To analyze the interaction between the zeolite-L/polymer brush
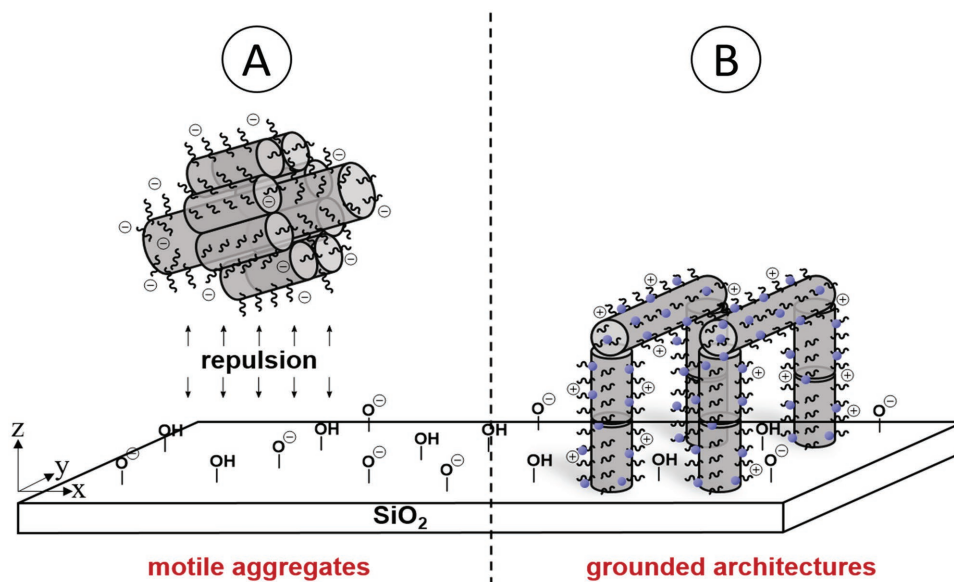

Figure 1. Two permanently assembled systems. Approach A: A hydrophobically functionalized structure with negative zeta potential not adhering to the cover glass substrate, thus a motile assembly. Approach B: A locally grounded architecture, built from subunits bearing hydrophilic functionalities (blue dots) with positive zeta potential.
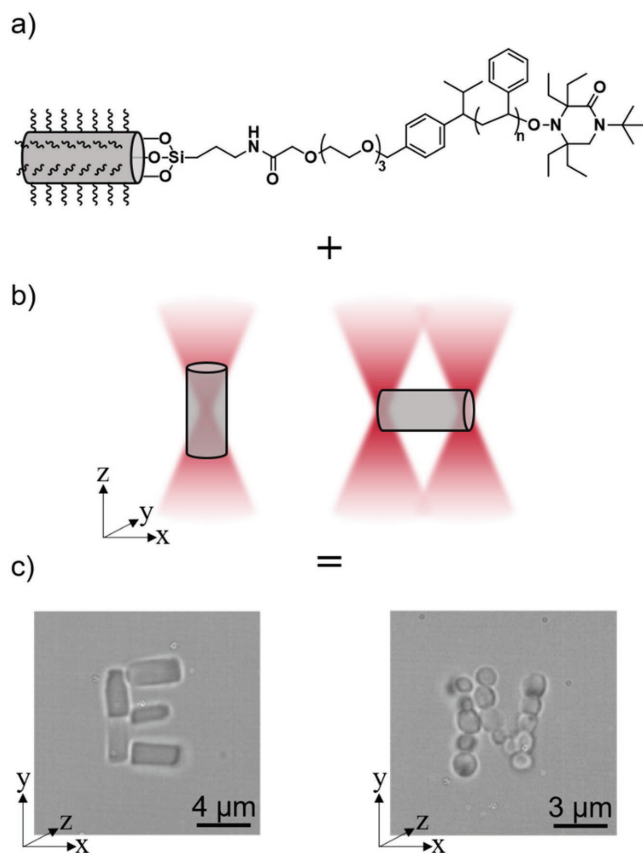
**ADVANCED
SCIENCE NEWS**

www.advancedsciencenews.com

Particle
& Particle Systems Characterization

www.particle-journal.com

a)

b)

c)

Figure 2. Combination of (a) zeolite-L-based polystyrene brush particles with, (b) optical trapping of these micro containers to create, and (c) motile permanent 2D micro structures.

particles, we trapped first several (7–25) particles, and subsequently positioned the particles next to each other to arrange them in specific configurations. Video S1 in the Supporting Information shows an example of HOT-assisted assembly of four zeolite-L/polymer brushes of 1 µm length. Owing to their elongated shape, zeolite-L crystals inherently align along the z-axis in optical traps, i.e., along the direction of propagation of the optical trapping beam (Figure 2b). The refractive index difference between the medium ($n_{DM} \approx 1.43$) and the zeolite-L crystal ($n_{zeolite} \approx 1.5$) resulted in stable trapping, ensuring a stable position of the zeolite-L crystal during assembly. Noteworthy, HOT allow creating asymmetric and anisotropic potentials by using tailored configurations of multiple traps, which allow precise rotation of elongated particles (Figure 2b). In this way, we are able to choose how zeolite-L crystals face each other, i.e., to investigate lateral–base, base–base, and lateral–lateral zeolite-L surface adhesion. In order to check whether the adhesion between particles was successful, we made sure that neither optical forces nor Brownian and hydrodynamic forces were able to induce disassembly of the zeolite-L structure. In total, we investigated $N = 126$ and $N = 84$ contact events for each particle size, achieving 100% efficiency of HOT-assisted assembly of zeolite-L/polymer hybrid particles in DMF for 1 µm crystals and $(66 \pm 9)\%$ for 4 µm crystals. Even though the mode of interaction between these particles is not fully understood yet, we

assume that it is based on a combination of hydrophobic and van der Waals forces as well as polymer strand entanglement.

The high assembly efficiencies of approach A allow readily building arbitrary 1D and 2D structures. Figure 2c shows two exemplary demonstrations in which zeolite-L/polymer brush particles were optomechanically assembled forming the letters "E" and "N," both consisting of five functionalized zeolite-L crystals of 4 µm length, and 15 crystals of 1 µm length, respectively. The hitherto used polystyrene functionalized zeolites did not adhere to the cover glass surface, since the cover glass, featuring free silanol groups, is negatively charged in a polar environment and these zeolites exhibited a negative zeta potential ($\zeta_{1 \mu m} = -48.1$ mV, $\zeta_{4 \mu m} = -59.0$ mV) as well. Thus, the glass substrate and these HOT-assembled microstructures repel due to mainly electrostatic forces. This feature prospects the use of crystals modified using approach A as suitable elements for building microtools that are able to be manipulated in the medium.

However, for some applications, one might require to fix the HOT-assembled microstructures on a substrate. For this purpose, in our approach B, we realized a hydrophilic functionalization, which features a positive zeta potential, and thus provides adhesion to the surface of, e.g., a glass substrate. In earlier works, we established a photo-postmodification approach as an efficient method to generate zeolite-L/polymer hybrids decorated with a variety of functional groups.[12] By means of the present approach, we extended the polymer shell to a random copolymer of styrene and a styrene-based acyloin monomer, which can be readily converted into a 4-amino-2,2,6,6-tetramethylpiperidinyloxylester (NH_2-TEMPO ester) moiety by activation with UV light ($\lambda = 365$ nm) and subsequent nitroxide trapping (**Figure 3**a).[33,34] Incorporating these amino and ester moieties leads to additional hydrogen bond formation, which can stabilize polymer and therefore crystal interactions. Crystals used in our experiments exhibit grafted-from, unmodified polymer strands of $M_n = 74$ kg mol^{-1} with a Đ = 1.21 (for 1 µm crystals) and $M_n = 85$ kg mol^{-1} with a Đ = 1.18 (for 4 µm crystals), respectively, which we assume to have slightly increased after photo-postmodification. Incorporation of styrene:photo-postmodifiable monomer amounts to 4:1 as determined by NMR spectroscopic analysis of the unbound polymer, which was generated during the polymer brush synthesis. The particles show zeta potentials of $\zeta_{1 \mu m} = +15.9$ mV and $\zeta_{4 \mu m} = +38.2$ mV in AFB (20×10^{-3} M, pH = 7.4, 25 °C) and therefore adhere on the negatively charged cover glass surface.

Following the sample preparation steps used in approach A, we proceeded with the demonstration of the HOT-assisted assembly of positively charged zeolite-L/polymer brush particles. We analyzed the success of the HOT-assisted assembly of $N = 96$ and $N = 90$ couples of zeolite-L crystals of 1 and 4 µm in length, respectively. The assembly efficiency resulted in $(89 \pm 5)\%$ for 1 µm crystals and 100% for 4 µm crystals. Figure 3b shows the result of HOT-assisted assembly of 19 elongated zeolite-L crystals functionalized with the copolymer shell of approach B, being arranged to form the logo of the University of Münster. For the assembly process, six crystals were trapped, connected to build a horizontal line, and finally fixed on the substrate glass surface. Subsequently, a second row of six crystals, two pairs of two crystals, and three single crystals were positioned
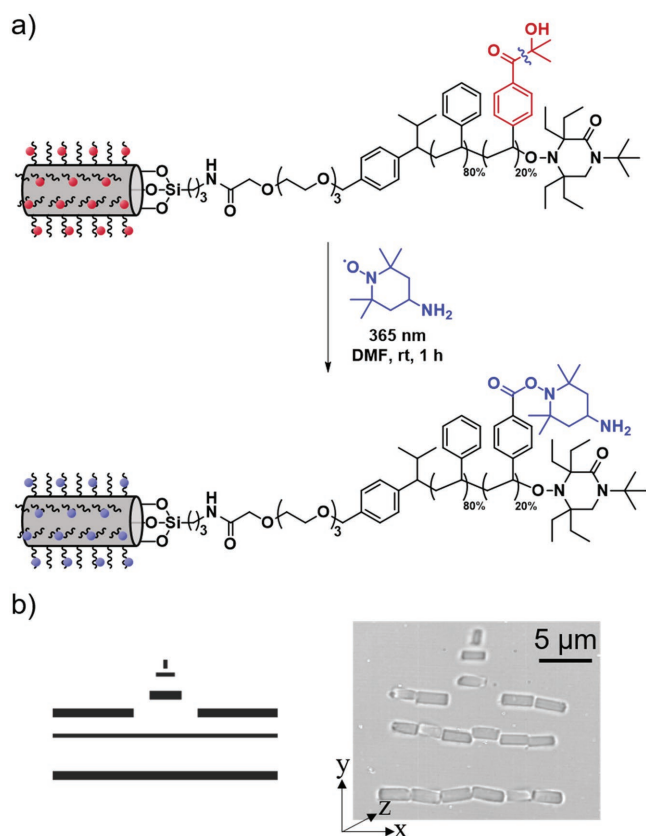
a)

b)

Figure 3. Demonstration of HOT-assisted 2D assembly of 4 μm zeolite-L/polymer hybrids. a) Structure and preparation of zeolite-L-based polymer brushes decorated with NH$_2$-TEMPO ester moieties (blue); b) Microscopy image of a micro structure (WWU logo) fixed on a cover glass.

and fixed on the surface by the same procedure to build the desired microstructure.

Finally, the versatility of the second approach B was further exploited to construct arbitrary 3D architectures. **Figure 4** shows ten HOT-assembled zeolite-L crystals of 1 μm length that feature a copolymer shell containing amino and ester groups within the polystyrene backbone. The zeolites were assembled in an arch-type structure by fixing first two crystals on the

surface, and then successively adding additional building blocks along the y–z plane. To demonstrate the bridge-form of the microstructure, an additional zeolite-L crystal (red circle) was trapped and guided below the permanently grounded arch (red arrows indicate direction of motion) (Video S2, Supporting Information).

In summary, we have introduced in this work two novel types of zeolite-L surface functionalization techniques that allow for optomechanically assisted assembly into permanently stable, arbitrary 1D, 2D, and 3D nano- and microarchitectures based on different crystal shapes and sizes. As a demonstration example, functionalized zeolite-L crystals were trapped and assembled with HOT. A soft, nonpolar polystyrene brush leads to hydrophobic interactions and polymer strand entanglement between single building blocks in polar media but no interaction and thus adhesion to the surrounding glass environment resulting in motile microstructures. A random copolymer shell consisting of polystyrene and a photo-postmodified styrene derivative bearing NH$_2$-TEMPO ester moieties serves for hydrophobic and hydrogen bonding interactions in combination with a positively charged particle surface that allow for particle–particle as well as particle-cover glass interactions and thus spatially fixed 3D microarchitectures.

This proof-of-concept approach is emphasizing the role of HOT as a powerful tool to realize optically assisted surface functionalization based on object interaction and adhesion, which in turn can be implemented as a screening method of self-assembly properties and strategies. Moreover, it paves the way to bottom-up construction of functional, designed nano- and microtools based on an readily accessible library of highly functionalized zeolite-L building blocks.[12] The assembly with further particles, or even living matter such as bacterial cells,[10–12,35,36] demonstrates the potential of the methods and pioneers applications in photonic structures, micromachines, or drug delivery in biomedical scenarios.

Experimental Section

Zeolite-L/Polymer Hybrid Preparation: Zeolite-L crystals were either purchased from Süd-Chemie (1.0–1.5 × 1.0 μm) or synthesized following reported procedures (4.0 × 1.0 μm).[37] Polymer brush particles were prepared and photo-postmodified according to previously published procedures.[12]
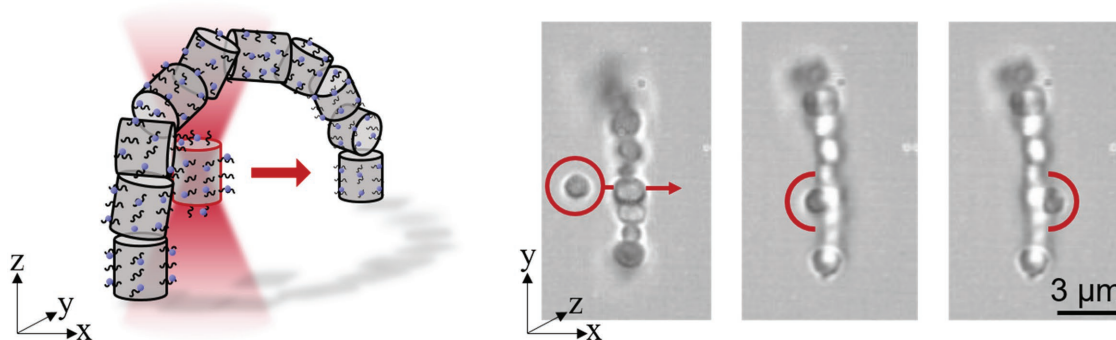

Figure 4. Ten zeolites with NH$_2$-functionalized polymer brushes build an arch-type structure. Left: Schematic representation of the 3D construction. Right: Top view of the actual experiment. The unbound crystal in the red circle is guided unhindered underneath the arch from left to right as indicated by the red arrow.

**ADVANCED
SCIENCE NEWS**
www.advancedsciencenews.com

Particle
& Particle Systems Characterization
www.particle-journal.com

GPC was carried out in degassed THF as eluent with a flow rate of 1.0 mL min^{-1} at room temperature on a system consisting of a Knauer HPLC Pump 64, a set of two PLgel 5 μm MIXED-C columns (300 × 7.5 mm, Polymer Laboratories) and a Shodex RI differential refractometer detector. Calibration was done with Varian polystyrene (PS) calibration kit, PL2010-0100, S-M-10, Lot 103. Signals of the PS standards ranged from M_n = 1530–1 319 000 g mol^{-1}. Data analysis was done with Polymer Standards Service WinGPC Compact V.7.20 software.

Zeta potential measurements were recorded with a DTS Zetasizer Nano ZS from Malvern. The measurements were performed in ammonium formate buffer (20 × 10^{-3} M pH = 7.4, 25 °C) at room temperature in a cell purged with dry methanol prior to the measurements. For interpretation, the Smoluchowski equation was applied. N,N-dimethylformamide, 99.8%, Extra Dry over Molecular Sieve, AcroSeal for HOT experiment dispersions was purchased from Acros Organics and used as received.

HOT Setup: For observation and optical control of the zeolite-L assemblies, an in-house developed HOT system was used that was implemented on the basis of a commercially available inverted fluorescence microscope (Eclipse Ti, Nikon) with a high numerical aperture microscope objective (Nikon Apo TIRF, 100×/1.49 Oil-immersion). The HOT system used as trapping light source a Nd:YVO$_4$ laser (Smart Laser Systems, Berlin, Germany) operating at a wavelength of λ = 1064 nm and of maximum output power 2.5 W. A half-wave plate (λ/2) and a polarizing beam splitter were placed at the beginning of the optical path in order to adjust the laser trapping power which was set to 200 mW measured at the back aperture of the inverted microscope. A beam expander, formed by microscope objective MO1 and lens L1, was used to illuminate the whole surface of a phase-only spatial light modulator (SLM) (1920 × 1080 pixels, "Pluto" LCOS display from Holoeye Photonics, Berlin, Germany). The SLM was used as a diffractive optical element to tailor the light field in several Gaussian shaped optical tweezers and to steer them 3D by displaying the phase pattern corresponding to the desired optical trapping configuration in the sample plane of the microscope.[38] For calculation of the phase pattern, a free software that was originally developed at the University of Glasgow, Scotland was adapted.[39] The SLM was imaged via a telescope, formed by lenses L2 and L3, onto the back aperture of the high numerical microscope objective MO2. A dichroic mirror was used to reflect the laser beam into the microscope objective MO2 and a filter (stop band at λ = 1064 nm) was used to separate the laser beam path from the observation path. The calculation of the holograms displayed in the SLM was performed with video repetition rate by using adequate computer hardware and thus providing dynamic on-line manipulation of optically trapped objects. Images of the assembly process and the subsequent motion of the bio-hybrid machine were acquired by a CCD.

Supporting Information

Supporting Information is available from the Wiley Online Library or from the author.

Conflict of Interest

The authors declare no conflict of interest.

[1] T. G. Leong, A. M. Zarafshar, D. H. Gracias, *Small* **2010**, *6*, 792.
[2] O. D. Velev, S. Gupta, *Adv. Mater.* **2009**, *21*, 1897.
[3] K. J. M. Bishop, C. E. Wilmer, S. Soh, B. A. Grzybowski, *Small* **2009**, *5*, 1600.
[4] G. Calzaferri, *Langmuir* **2012**, *28*, 6216.
[5] K. B. Yoon, *Acc. Chem. Res.* **2007**, *40*, 29.
[6] M. Becker, L. De Cola, A. Studer, *J. Mater. Chem. C* **2013**, *1*, 3287.
[7] R. M. Barrer, H. Villiger, *Z. Kristallogr. - New Cryst. Struct.* **1969**, *128*, 352.
[8] H. Lülf, A. Bertucci, D. Septiadi, R. Corradini, L. De Cola, *Chem. - Eur. J.* **2014**, *20*, 10900.
[9] M. Veiga-Gutiérrez, M. Woerdemann, E. Prasetyanto, C. Denz, L. De Cola, *Adv. Mater.* **2012**, *24*, 5199.
[10] Z. Popović, M. Otter, G. Calzaferri, L. De Cola, *Angew. Chem.,– Int. Ed.* **2007**, *46*, 6188.
[11] Á. Barroso, S. Landwerth, M. Woerdemann, C. Alpmann, T. Buscher, M. Becker, A. Studer, C. Denz, *Biomed. Microdevices* **2015**, *17*, 1.
[12] T. Buscher, A. Barroso, C. Denz, A. Studer, *Polym. Chem.* **2015**, *6*, 4221.
[13] A. Szarpak-Jankowska, C. Burgess, L. Decola, J. Huskens, *Chem. - Eur. J.* **2013**, *19*, 14925.
[14] M. Becker, L. De Cola, A. Studer, *Chem. Commun.* **2011**, *47*, 3392.
[15] V. Vohra, A. Bolognesi, G. Calzaferri, C. Botta, *Langmuir* **2010**, *26*, 1590.
[16] S. Suárez, A. Devaux, J. Buñuelos, O. Bossart, A. Kunzmann, G. Calzaferri, *Adv. Funct. Mater.* **2007**, *17*, 2298.
[17] A. Devaux, Z. Popovic, O. Bossart, L. De Cola, A. Kunzmann, G. Calzaferri, *Microporous Mesoporous Mater.* **2006**, *90*, 69.
[18] S. Huber, G. Calzaferri, *Angew. Chem., Int. Ed.* **2004**, *43*, 6738.
[19] J. M. Beierle, R. Roswanda, P. M. Erne, A. C. Coleman, W. R. Browne, B. L. Feringa, *Part. Part. Syst. Charact.* **2013**, *30*, 273.
[20] Z. Popović, M. Busby, S. Huber, G. Calzaferri, L. De Cola, *Angew. Chem., Int. Ed.* **2007**, *46*, 8898.
[21] B. Schulte, M. Tsotsalas, M. Becker, A. Studer, L. De Cola, *Angew. Chem., Int. Ed.* **2010**, *49*, 6881.
[22] M. Woerdemann, S. Gläsener, F. Hörner, A. Devaux, L. D. De Cola, C. Denz, *Adv. Mater.* **2010**, *22*, 4176.
[23] J. S. Oh, Y. Wang, D. J. Pine, G. R. Yi, *Chem. Mater.* **2015**, *27*, 8337.
[24] G. A. Williams, R. Ishige, O. R. Cromwell, J. Chung, A. Takahara, Z. Guan, *Adv. Mater.* **2015**, *27*, 3934.
[25] J. Song, G. Niu, X. Chen, *Bioconjugate Chem.* **2017**, *28*, 105.
[26] M. G. Moffitt, *J. Phys. Chem. Lett.* **2013**, *4*, 3654.
[27] Y. Tan, W. Zhang, Y. Li, Y. Xia, K. Sui, *RSC Adv.* **2016**, *6*, 92305.
[28] K. Liu, A. Lukach, K. Sugikawa, S. Chung, J. Vickery, H. Therien-Aubin, B. Yang, M. Rubinstein, E. Kumacheva, *Angew. Chem., Int. Ed.* **2014**, *53*, 2648.
[29] A. Piqué, R. C. Y. Auyeung, H. Kim, N. A. Charipar, S. A. Mathews, *J. Phys. D. Appl. Phys.* **2016**, *49*, 223001.
[30] J. Fischer, M. Wegener, *Laser Photonics Rev.* **2013**, *7*, 22.
[31] H. M. Saavedra, T. J. Mullen, P. Zhang, D. C. Dewey, S. A. Claridge, P. S. Weiss, *Rep. Prog. Phys.* **2010**, *73*, 36501.
[32] Y. L. Zhang, Q. D. Chen, H. Xia, H. B. Sun, *Nano Today* **2010**, *5*, 435.

[33] A. Mardyukov, A. Studer, *Macromol. Rapid Commun.* **2013**, *34*, 94.

[34] A. Mardyukov, Y. Li, A. Dickschat, A. H. Schaefer, A. Studer, *Langmuir* **2013**, *29*, 6369.

[35] A. Barroso, M. C. Grüner, T. Forbes, C. Denz, C. A. Strassert, *ACS Appl. Mater. Interfaces* **2016**, *8*, 15046.

[36] F. Hörner, M. Woerdemann, S. Müller, B. Maier, C. Denz, *J. Biophotonics* **2010**, *3*, 468.

[37] A. Z. Ruiz, D. Brühwiler, T. Ban, G. Calzaferri, *Monatsh. Chem.* **2005**, *136*, 77.

[38] J. Liesener, M. Reicherter, T. Haist, H. J. Tiziani, *Opt. Commun.* **2000**, *185*, 77.

[39] R. W. Bowman, G. M. Gibson, A. Linnenberger, D. B. Phillips, J. A. Grieve, D. M. Carberry, S. Serati, M. J. Miles, M. J. Padgett, *Comput. Phys. Commun.* **2014**, *185*, 268.